17th World Conference on Earthquake Engineering, 17WCEE
Sendai, Japan - September 13th to 18th 2020

SEISMIC COLLAPSE EVALUATION ON IRREGULAR STEEL MOMENT RESISTING FRAMES WITH STRUCTURE-SOIL INTERACTION

Y. Li[(1)], Y. Bai[(2,3*)], and Z. Tang[(4)]

[(1)] *Graduate student, Xi'an Jiaotong University, 1162923235@qq.com*
[(2)] *Professor, School of Civil Engineering, Chongqing University, bai.yongtao@cqu.edu.cn*
[(3)] *Humboldt fellow, Institute for Risk and Reliability, Leibniz Universität Hannover, baiyongtao@gmail.com*
[(4)] *Associate professor, Beijing University of Technology, tzy@bjut.edu.cn*

Abstract

In this paper, the real-time dynamic substructuring tests of the shaking table are performed, including four structural systems: steel moment-resisting frame (SMRF), frame with equipment (SMRF-EM), frame with foundation soil (SMRF-S) and frame with equipment and foundation soil (SMRF-EM-S). The equipment and the upper steel moment-resisting frame are experimental substructures, and the foundation soil is a numerical substructure. The displacement response of SMRF-EM-S is studied from minor earthquakes to rare earthquakes. As the earthquake intensity increases, the damage and lateral displacement of the structure are concentrated downwards, which eventually causes the lateral collapse of the bottom story. The effects of equipment and foundation soil on structural acceleration and deformation response have been studied. During the minor earthquakes, the equipment increases the acceleration response of the top story of the structure. During the medium earthquakes, the equipment even reduces the acceleration response of the structure, and the foundation soil always reduces the overall acceleration response of the structure. In addition, equipment increases the seismic displacement response of the structure and the risk of structural collapse, while the foundation soil has a shock-absorbing effect.

Keywords: Shaking table test, *Sub-structure*, *Steel moment-resisting frame, Mass irregularity, Structure-soil interaction, Seismic collapse*

1. Introduction

In seismic-prone areas, steel moment-resisting structure buildings have been widely constructed for its ductile seismic performance. However, the local damage of the nodes and components of the steel structure will still occur under strong earthquakes. The failure of beam-column joints or the strength degradation caused by local buckling of beam-columns may increase the risk of structural collapse[1]. For instance, severe damage to beam-column joints, and even brittle fracture of steel columns and the collapse of weak stories were observed during the Northridge earthquake (1994) and the Hyogoken-Nanbu earthquake (1995). Moreover, the effects of mass irregularity and the structure-soil interaction on seismic collapse performance are still open topics for the seismic design to prevent collapse.

Limited experimental studies have been performed on the seismic collapse of steel moment frames. Suita et al. (2008) have experimentally investigated the collapse mechanism of a full-scale SMRF designed with slender beam-columns[2]. Lignos et al. (2011) conducted shaking table tests of two 4-story steel moment-resisting frames with a 1: 8 scale model, demonstrating that the structure may undergo lateral collapse due to the actual combined effect of the structural frame and seismic ground motion[3]. They found that structural damage was one of the main causes of steel moment-resisting frame collapse. Li et al. (2003) based on the shaking table test of the structure-equipment combination system, concluded that: The change in the frequency spectrum of the combined system is the essential reason for the difference in structural response. Different seismic inputs have a significant impact on the seismic response of the combined structure-equipment system[4]. Shang and Chen (2012) completed a dynamic test of a 1: 4 steel frame in a soil trench and they found that the soil foundation has some influence on the seismic response of steel frames[5]. Guo et al. (2017) applied and developed substructure test technology, which overcomes the shortcomings of traditional soil-knot interaction test research and provides convenience for soil-knot interaction test research[6].

In this paper, the real-time dynamic substructuring shaking table tests are used to study the response of steel frames under different ground motions. The equipment and the upper steel moment-resisting frame are experimental substructures, and the foundation soil is a numerical substructure. The seismic response of four structural systems (SMRF, SMRF-EM, SMRF-S, and SMRF-EM-S) and the collapse mechanism of structures under earthquakes are studied. The effects of auxiliary equipment and foundation soil on the seismic acceleration and deformation response of the structure are clarified.

2. Real-time dynamic substructuring test

2.1 Numbering of subsections

This experiment is a real-time dynamic substructuring experiment, dividing into numerical substructure (calculation substructure) and experimental substructure. The experimental system is shown in Figure 1. There are also control systems and acquisition systems in addition to the substructure. The numerical substructure calculation and controller design are completed by SIMULINK simulation software installed on a professional engineering control computer, which can ensure that the calculation module runs in a real-time environment. The test objects include structure, equipment and foundation soil. The structure is a four-story steel moment-resisting frame, the equipment is set on the top story of the frame, and the foundation soil is the third type of site soil. The equipment and structure are experimental substructures, and the foundation soil is a numerical substructure.

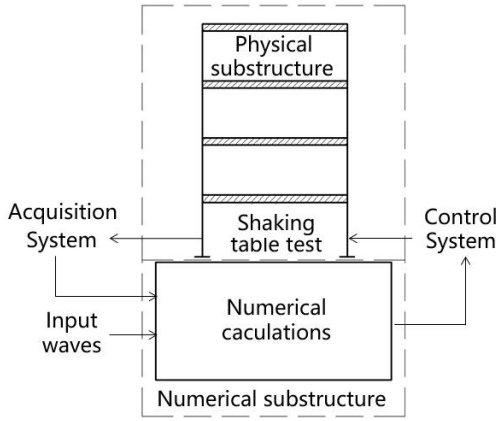

Fig. 1 –Real-time dynamic substructuring shaking table test system

2.2 Test model

2.2.1 Physical substructure

The upper steel frame and auxiliary equipment are physical substructures, and the specific parameters of the physical model are as follows. The model is a 1: 5 scale, single-span, four-story steel moment-resisting frame, as shown in Figure 2. The distance between the horizontal and vertical axes is 1.60m. The height of the first floor is 0.68m, the height of the standard floor (the remaining three floors) is 0.63m, and the total height of the model structure is 2.57m. Bi-directional beams are arranged in a cross shape to sustain vertical masses. Beam and column cross-sections are H-shaped (HN100×45×6×8), and the yield strength of beam and column materials is 339.6MPa. The equipment uses a circular steel tube design, the material yield strength is 421.4MPa. It is connected to the top floor of the steel frame structure by four bolts on the bottom plate. Floor masses are 1700kg, 1700kg, 1700kg, and 1540kg, respectively, and equipment weight is 90kg.

The structure of the connection is shown in Figure 3. The connection between the beam flange and the column is welded. The weld is a fully welded groove butt weld, and the connection weld between the beam web and the column is a double-sided fillet weld. Beam-column joints are provided with two kinds stiffeners, the dimensions are b×h=19.5mm×84mm and b×h=19.5mm×113mm, and the thickness is 8mm. The secondary beam and the main beam web are connected in the form of double-sided fillet welds, and a fully welded groove butt weld is used to connect the flange to the flange.

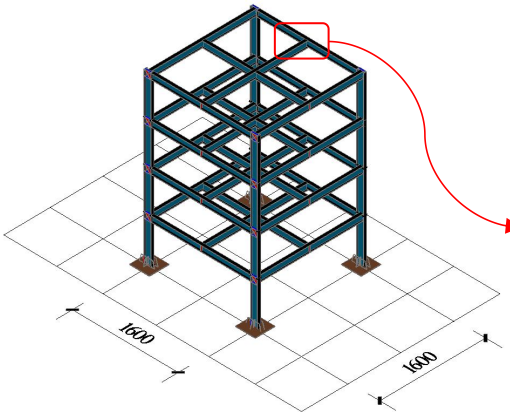

Fig. 2 –Perspective view of SMRF

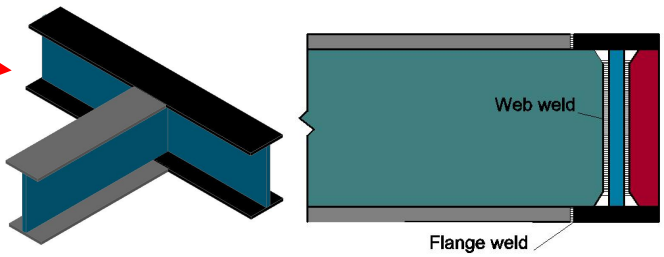

Fig. 3 –Beam and column connections

2.2.2 Numerical model for soil foundation

The foundation and soil structure are numerical substructures. The soil's excellent periodic similarity ratio is applied to design the model soil, retaining the main characteristics of the original site soil, making the model similar to the prototype[7]. The soil finite element model established by the general finite element

software ANSYS according to the test design requirements. The soil finite element model is an eight-node solid element, and the deformation of the soil model is mainly the translational deformation in the x-direction. The soil model is fixed at the bottom and surrounded by viscoelastic boundaries. The total size of the model is 30m×15m×15m, as shown in Figure 4. The embedded concrete foundation measures 2.2m×2.2m×0.4m and is located in the middle. The size of the embedded concrete foundation is 2.2m×2.2m×0.4m, which is located in the middle, the buried depth is 0.4m, the elastic modulus is 35200MPa, the density is 2650kg/m^3, and the damping ratio is 0.25. The foundation soil is divided into three layers, and the specific parameters are shown in Table 1.

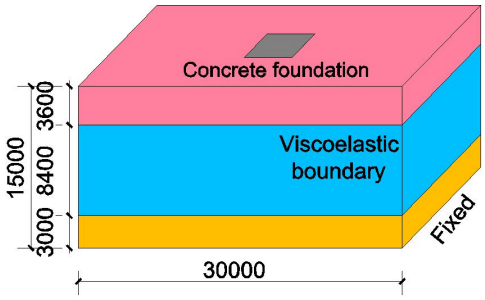

Fig. 4 –Foundation soil model

Table 1 – Soil parameters of each layer

Layer number	Depth (m)	Density (kg/m^3)	Elastic modulus (MPa)	Shear wave velocity (cm/s)	Damping ratio
1	0~3.6	1730	21.1	6.8×10^3	0.35
2	3.6~12	1950	56.4	1.05×10^4	0.35
3	12~15	2030	337	2.53×10^4	0.35

2.3 Input wave and test scheme

Due to the uncertainty in the actual earthquake, the loading direction of the test is adopted along the direction of the structure with weak seismic resistance. In this test, the El-Centro wave, Synthetic wave, and Tianjin wave are selected. The intensity of the ground motion ranges from minor earthquakes to rare earthquakes. There are four types of structural systems: steel moment-resisting frame(SMRF), frame with equipment (SMRF-EM), frame with foundation soil(SMRF-S) and frame with equipment and foundation soil(SMRF-EM-S). Figure 5 is the acceleration time history curve of the synthetic wave, PGA is 0.7m/s^2, 2m/s^2 and 3m/s^2. The acceleration response spectra of input seismic waves are shown in Figure 6. Based on seismic code GB 50011-2010, the seismic design of the test site is grouped into the first group, the site soil is the third group, and the seismic fortification intensity is 8 degrees. The light-grey curve is the design response spectrum under the frequent earthquakes (50% overrun probability is 63%), and the dark-grey curve is the design response spectrum under the rare earthquakes (50% overrun probability 2%). The response spectra of the three waves are close to the designed response spectra of frequent earthquakes, while the response spectra of El-Centro waves and synthetic waves in the rare earthquake stage and Tianjin waves in the medium earthquake stage are close to the designed response spectra of rare earthquakes. The detailed loading scheme is shown in Table 2.

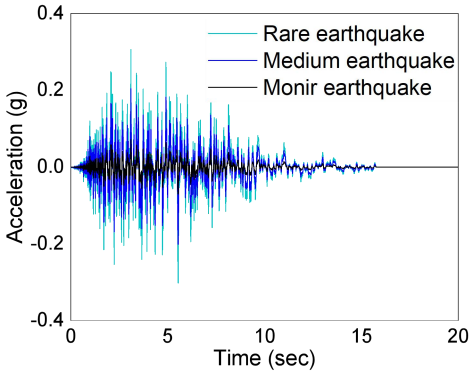

Fig. 5 –Scaled time-history synthetic waves

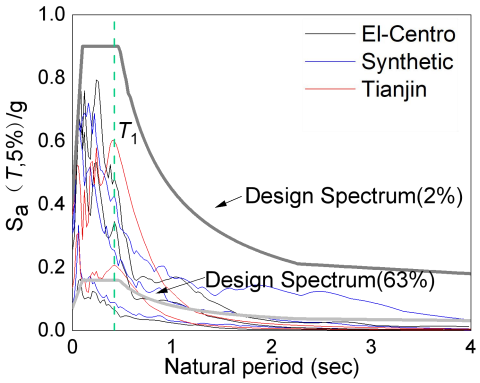

Fig. 6 –Input seismic waves response spectra

Table 2 –Earthquake detailed loading scheme

Earthquake intensity	Waves	Acceleration	Structure type
Minor earthquake	El-Centro wave	0.7 m/s^2	SMRF SMRF-EM SMRF-S SMRF-EM-S
	Synthetic wave		
	Tianjin wave		
Medium earthquake	El-Centro wave	2.0 m/s^2	SMRF SMRF-EM SMRF-S SMRF-EM-S
	Synthetic wave		
	Tianjin wave		
Rare earthquake	El-Centro wave	3.0 m/s^2	SMRF-EM-S
	Synthetic wave		

3. Test results

3.1 Acceleration amplitude

Take the quotient of the acceleration response peak value of each measurement point and the acceleration peak value measured on the table, and the calculated value is the acceleration amplification factor at the measurement point[8].

Figures 7 and 8 show the distribution of the acceleration amplification factor of each storey of SMRF under the incremental seismic ground motions. The black curve is the El-Centro wave, the blue curve is the Synthetic wave, and the red curve is the Tianjin wave. In the minor earthquake stage, the changes in the acceleration amplification factors of the various floors under the three types of seismic waves are inconsistent, and the structures under different seismic waves show different acceleration responses. The seismic energy at this stage is dissipated by damping, and the internal energy dissipation component is low. And it also shows that no damage occurs inside the structure. The changes in the acceleration amplification factors are consistent, indicating that the internal energy consumption component of the structure has increased, and the structural damping ratio has increased. This phenomenon is caused by plasticity, damage, and stiffness degradation that occur inside the structure.

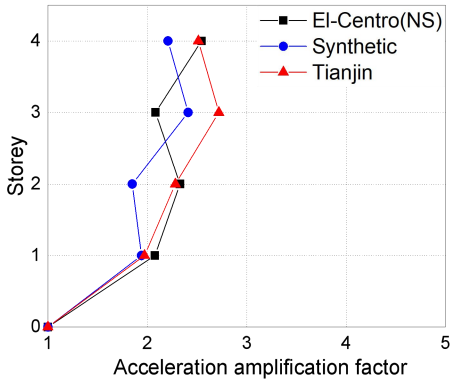

Fig. 7 –Factor under minor earthquake of SMRF

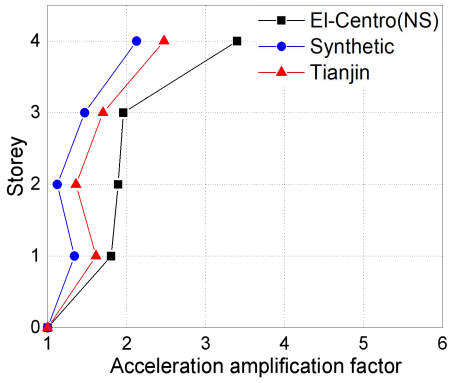

Fig. 8 –Factor under medium earthquake of SMRF

Figures 9 and 10 show the distribution of the average acceleration amplification factors of each structural system along the floors during the minor and medium earthquakes. The black, red, blue, and green curves correspond to SMRF, SMRF-EM, SMRF-S, and SMRF-EM-S. During minor earthquakes, the trends of SMRF and SMRF-S are consistent, and the trends of SMRF-EM and SMRF-EM-S are consistent. The equipment increases the acceleration response of the top floor of the structure, and the soil reduces the acceleration response of the entire structure. During medium earthquakes, the distribution of the four types of structures tends to be the same. The SMRF's acceleration response is the largest, and the soil and equipment reduce the acceleration response of SMRF.

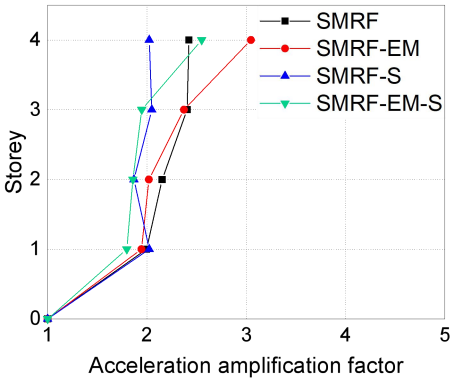

Fig. 9 –Average factor under minor earthquakes

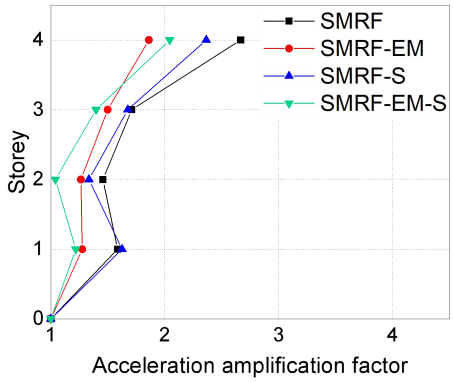

Fig. 10 –Average factor under medium earthquakes

3.2 Inter-storey drift ratios

Figures 11(a) and 11(b) are SMRF-EM-S's inter-storey drift ratios under the action of EL-Centro waves and Synthetic records. The black, blue, and red curves represent minor, medium, and rare earthquakes. Under the minor earthquakes, the inter-storey drift ratio of each floor of SMRF-EM-S is linear and less than 1/250 of the calculation of the elastic stage specified in the specification. That shows that the structure is in the elastic phase. With the increase of earthquake intensity, the inter-storey drift ratio of each floor increases. During medium earthquakes, the inter-storey drift ratio of some floors exceeds the elastic limit, and some parts of the structure enter into plasticity. Earthquake intensity continues to increase, damage and lateral displacements are concentrated towards the bottom floor, and lateral displacement of the bottom floor is significantly increased. During the rare earthquakes, the lateral displacement of the bottom floor exceeds the prescribed collapse limit, and the structure occurs lateral collapse.

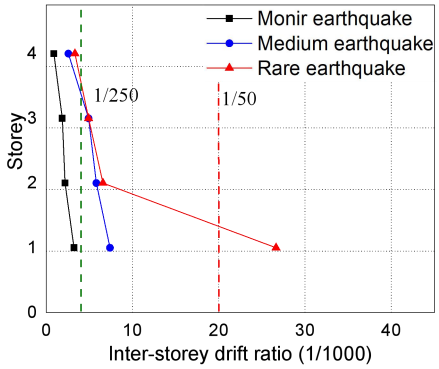

(a) El-Centro wave

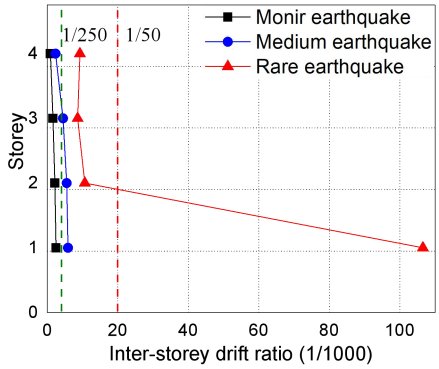

(b) Synthetic wave

Fig. 11 – Inter-storey drift ratio of SMRF-EM-S

Figure 12 shows the distribution of the inter-storey drift ratios of SMRF-EM under Tianjin waves. During the minor earthquakes, some parts of the structure have already entered the plastic phase, and the structure collapses during the medium earthquakes. One of the reasons is that the corresponding Tianjin wave earthquake response at the natural vibration period of the structure is larger.

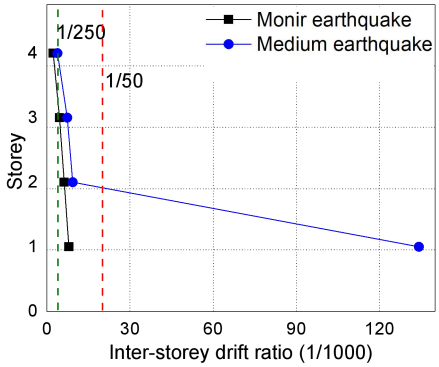

Fig. 12 – Inter-storey drift ratio of SMRF-EM under Tianjin wave

Figures 13 and 14 show the average inter-storey drift ratios under minor and medium earthquakes, respectively. The black, red, blue, and green curves correspond to SMRF, SMRF-EM, SMRF-S, and SMRF-EM-S. It is noted that the inter-storey drift ratio of SMRF-EM is greater than SMRF, the inter-storey drift ratios angle of SMRF-S is less than SMRF. Equipment increases the drift response of the structure, while the foundation soil reduces the seismic deformation of the upper structure and has a damping effect. That explains the collapse of SMRF-EM. Under the earthquakes, on the one hand, due to the flexibility of the soil, on the other hand, the energy in the superstructure is transmitted to the soil by means of scattering[9-10]. Therefore, the soil-structure interaction will increase the vibration period and damping of the structural system, which will lead to a decrease in the seismic response of the structure.

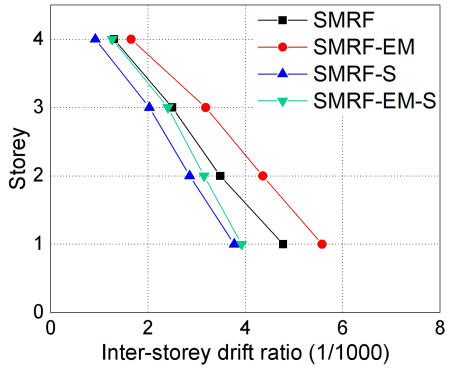

Fig. 13–Average drift ratio under minor earthquakes

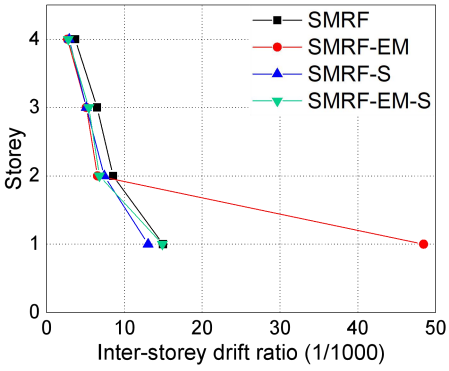

Fig. 14 –Average drift ratio under medium earthquakes

4. Conclusions

In this paper, the real-time dynamic substructuring tests on shaking table are carried out, including four types of structures, i.e. SMRF, SMRF-EM, SMRF-S, and SMRF-EM-S to evaluate the seismic collapse capacity of irregular SMRFs with structure-soil interaction. During the minor earthquakes, the equipment increases the acceleration response of the top story of the structure. During the medium earthquakes, the equipment even reduces the acceleration response of the structure, and the foundation soil always reduces the overall acceleration response of the structure. Under El-Centro and Synthetic waves, the upper steel frame of SMRF-EM-S remains in elasticity under the minor earthquakes. During the medium earthquakes, some parts of the upper steel frame enter into plasticity, and the damage and lateral displacement of the structure are concentrated downwards. Eventually, the lateral collapse of the bottom story occurs during the rare earthquakes. However, under the Tianjin wave, SMRF-EM even collapses during the medium earthquakes. The equipment increases the deformation response of the structure, while the foundation soil reduces the seismic deformation of the upper structure with the damping effect. That explains the collapse of SMRF-EM.

5. Acknowledgements

This study is partially supported by the National Natural Science Foundation of China (51508459 and 51978016), and the corresponding author is greatly grateful to the Alexander von Humboldt Stiftung-Foundation (1196752).

6. Copyrights

7. References

[1] Bai Y, Lin, X. (2015): Numerical simulation on seismic collapse of thin-walled steel moment frames considering post local buckling behavior, *Thin-Walled Structures*, 94, 424-434.

[2] Suita K., Yamada S., Tada M., Kasai K., Matsuoka Y., Shimada Y. (2008): Collapse Experiment on Four-Story Steel Moment Frame: Part 2. *Proc. 14th World Conf. Earthquake Eng*: Beijing, China.

[3] Lignos D G, Krawinkler H, Whittaker A S. (2011): Prediction and validation of sidesway collapse of two scale models of a 4-story steel moment frame. *Translated World Seismology*, 40(7), 807-825.

[4] Li J, Chen H, Sun Z. (2003): Experimental Study on Structure-Equipment Dynamic Interaction. *Engineering Mechanics*, 20(1), 157-161.

[5] Shang S, Chen W. (2012): Experimental Investigation of Soil-structure Interaction on the Excitation Test of 1:4 Scaled Steel Frame-raft Foundation Model. *Journal of Sichuan University*, 44(6), 27-33.

[6] Guo J, Tang Z, Li Y, et al. (2017): The simulation of soil structure interaction baced on substructuring testing. *Engineering Mechanics*, 34, 214-219.

[7] Jiang X, Xu B, Li Z. (2010):Similitude laws and its application in shaking table test of soil-pile-structure interaction system. *Journal of Vibration Engineering*, 23(2), 225-229.

[8] Huang B， Lu W， Chen S. (2017):Shaking table tests of RC frame under consecutive strong ground motion excitations. *Journal of Building Structures*, 38(9), 84-93

[9] Lv X, Chen Y, Chen B, et al. (2000): Shaking table testing of soil-structure interaction system. *Earthquake Engineering and Engineering Vibration*, 20(4), 20-29.

[10] Chen G, Wang Z, Zai Z. (2001): Shaking table model testing of structure suppressing vibration control including soil-structure interaction effects. *Earthquake Engineering and Engineering Vibration*, 21(4), 117-127.

